

Pt decorated POMOFs-derived constructions for efficient electrocatalytic hydrogen evolution

Wei Jia^{a,*}, Juanli Zhang^a, Zhenjiang Lu^a, Shiqiang Wang^a, Shizhan Feng^a

^aKey Laboratory of Energy Materials Chemistry, Ministry of Education; Key Laboratory of Advanced Functional Materials, Autonomous Region; Institute of Applied Chemistry, Xinjiang University, Urumqi, Xinjiang 830046, P.R. China

Experimental Section

Chemicals: Hydrochloroplatinic acid (H_2PtCl_6) and copper (II) acetate monohydrate ($(\text{CH}_3\text{COO})_2\text{Cu}\cdot\text{H}_2\text{O}$) were purchased from Sinopharm Chemical Reagent Co. Ltd. 12-molybdophosphoric acid hydrate ($\text{H}_7(\text{P}(\text{Mo}_2\text{O}_7)_6\cdot x\text{H}_2\text{O})$), L-glutamic acid ($\text{C}_5\text{H}_9\text{NO}_4$), 1,3-propanediol ($\text{C}_3\text{H}_8\text{O}_2$), and 1,3,5-benzenetricarboxylic acid ($\text{C}_9\text{H}_6\text{O}_6$) were purchased from Alfa Aesar. All the chemicals were used as received without further purification.

Synthesis of NENU-5 nano-octahedrons: In a typical synthesis, 182 mg of copper(II) acetate monohydrate, 90.8 mg of L-glutamic acid, and 300 mg of 12-molybdophosphoric acid hydrate were dissolved in 30 mL of deionized water and stirred for 20 min at room temperature. Then 122 mg of 1,3,5-benzenetricarboxylic acid dissolved in 30 ml of ethanol was poured into the above solution under continuous stirring. The solution immediately turns turbid due to the rapid formation of NENU-5 nanocrystals. After stirring for overnight at ambient condition, the green precipitates were collected by centrifugation and washed three times with ethanol. The products were dried at 60 °C for 12 h.

Synthesis of porous Mo_2C nano-octahedrons: The NENU-5 nano-octahedrons were heated in a tube furnace in Ar flow with a ramp rate of 5 °C min⁻¹, maintained at 800 °C for 6 h and then cooled down naturally. The as-prepared sample was denoted as Cu/ Mo_2C . The Cu nanoparticles were removed by dispersing in 0.1 M FeCl_3 aqueous solution at ambient condition for 5 h. The resulting porous Mo_2C nano-octahedrons were collected by centrifugation, washed with deionized water repeatedly and then dried at 60 °C overnight.

*Corresponding author.

E-mail address: jia3816892@163.com (W. Jia)

Synthesis of Pt-Cu/Mo₂C: In a typical synthesis, 50 mg of the as-prepared Cu/Mo₂C sample, different amounts of H₂PtCl₆ and 6 mL of 1,3-propanediol were added into 30 mL airtight vial, then the mixture was ultrasonicated for 30 minutes. Subsequently, the resulting homogeneous mixture was heated at 165 °C for 10 h in an oil bath. Then it was cooled to room temperature, collecting products by centrifugation and washing three times with ethanol/acetone mixture. The sample is denoted as Pt-Cu/Mo₂C-X, where X (=100, 300, 500, 700, 900) represents the adding amount of H₂PtCl₆ (μL, 0.1 g mL⁻¹), and Pt-Cu/Mo₂C is referred to Pt-Cu/Mo₂C-500.

Synthesis of Pt/Mo₂C: 50 mg of the as-prepared Mo₂C sample and 500 μL of H₂PtCl₆ (0.1 g mL⁻¹) were added into 6 mL of 1,3-propanediol in 30 mL airtight vial, then ultrasonically treated for 30 minutes. Subsequently, the resulting homogeneous mixture was heated at 165 °C for 10 h in an oil bath. Then it was cooled to room temperature, collecting products by centrifugation and washing three times with ethanol/acetone mixture.

Characterizations

The morphologies and structures of the as-prepared samples were observed by transmission electron microscopy (TEM, JEM-2100F, Japan) and scanning electron microscopy (SEM, S-4800, Japan) equipped with energy dispersive X-ray spectroscopy (EDX). X-ray diffraction (XRD) measurements were performed on a D8 Bruker diffractometer with Cu Kα (λ=1.5418 Å) radiation to determine the crystallite structures. X-ray photoelectron spectroscopy (XPS) measurements were carried out using an ESCALAB 250Xi electron spectrometer (Thermo Fisher Scientific) with Al Kα radiation. N₂ adsorption-desorption was measured with Micromeritics ASAP 2020M to obtain the surface area and pore size distributions. The Pt loading amount of catalysts was determined by Agilent 5110 inductively coupled plasma optical emission spectroscopy (ICP-OES).

Electrochemical measurements

Hydrogen evolution reaction (HER) measurements were performed on WaveDrive 20 (PINE Research Instrumentation) at room temperature using a standard three-electrode system with Ag/AgCl (3 M KCl) as reference electrode, graphite rod as counter electrode, and catalyst-modified glassy-carbon rotating disk electrode (RDE)

as working electrode. The Ag/AgCl electrode was calibrated with respect to a reversible hydrogen electrode (RHE, $E_{\text{(RHE)}} = E_{\text{(Ag/AgCl)}} + 0.059\text{pH}$). 5.0 mg of catalyst and 20 μL of 5 wt% Nafion solution were dispersed in 980 μL of water/isopropanol mixture (3:1, v/v) with sonication for about 1 h to form homogeneous ink. Then 10 μL of the ink was loaded onto a RDE of 5 mm in diameter (loading $\sim 0.255 \text{ mg cm}^{-2}$) and dried at ambient temperature. The HER test was carried out in N_2 -saturated 0.5 M H_2SO_4 solution. Linear sweep voltammetry (LSV) was conducted at a scan rate of 5 mV s^{-1} . The durability test was carried out by taking continuous potential cycling in the range of -0.1 to 0.2 V (versus RHE) at a scan rate of 100 mV s^{-1} . After potential cycling, the LSV curves were recorded at a scan rate of 5 mV s^{-1} . Electrochemical impedance spectroscopy (EIS) measurements were performed in 0.5 M H_2SO_4 over the frequency ranging from 100 kHz to 0.1 Hz with an amplitude of 5 mV at the open-circuit voltage. To estimate the electrochemical surface area (ECSA) of the catalysts, cyclic voltammetry (CV) measurements were conducted in the potential range of 0 to 1.4 V vs. RHE in 0.5 M H_2SO_4 solution at a scan rate of 50 mV s^{-1} . The ECSA was obtained by integrating the H-desorption region of Pt species and dividing the resulting coulombic charge by $210 \text{ C cm}_{\text{Pt}}^{-2}$.

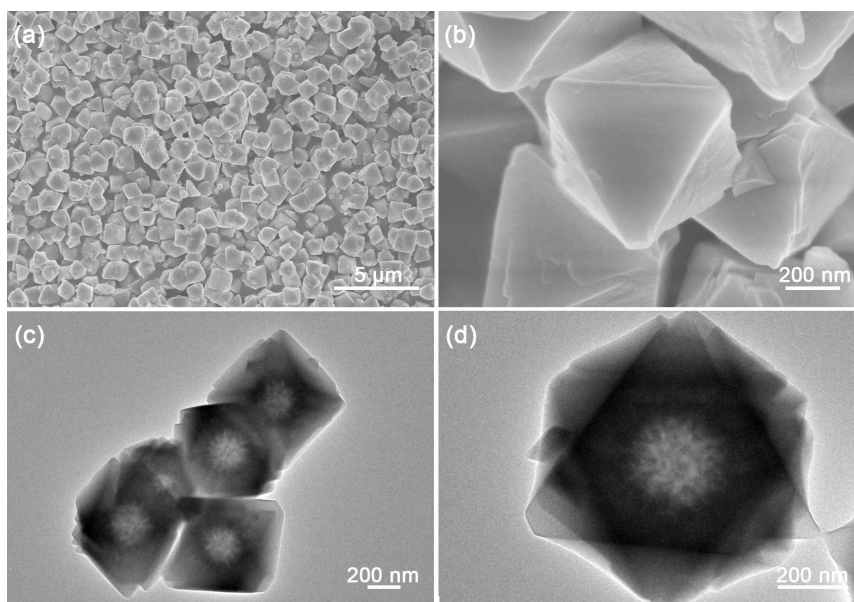


Fig. S1 (a-b) SEM images and (c-d) TEM images of NENU-5.

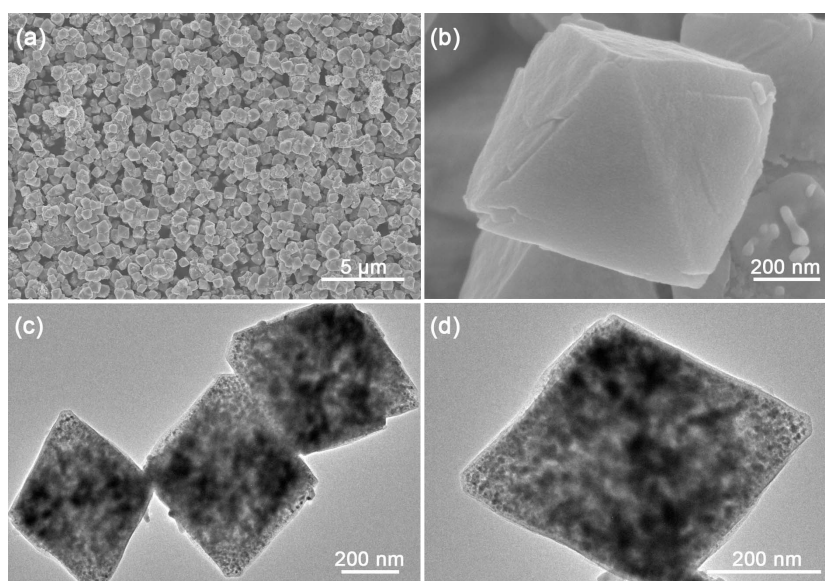


Fig. S2 (a-b) SEM images and (c-d) TEM images of Cu/Mo₂C.

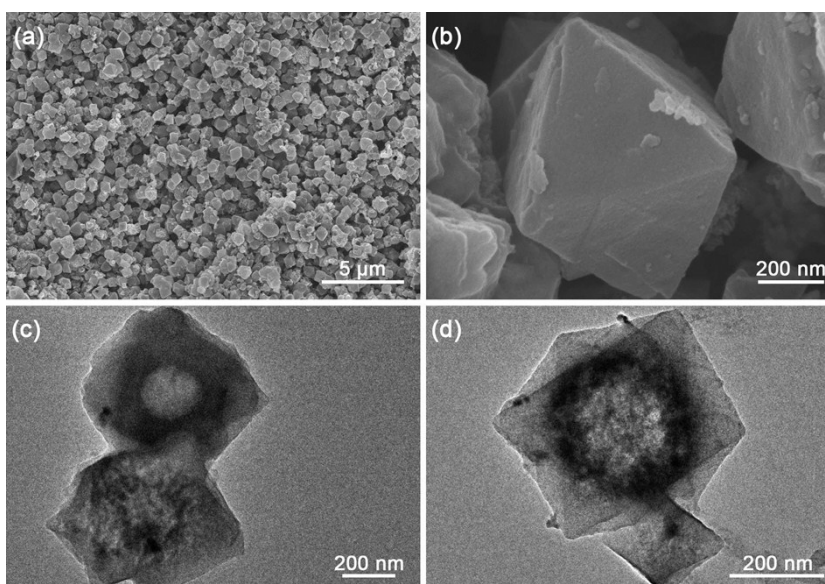


Fig. S3 (a-b) SEM images and (c-d) TEM images of Mo₂C.

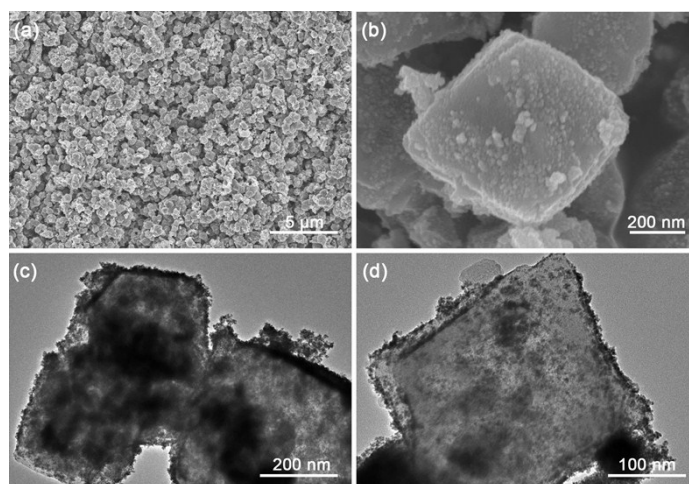


Fig. S4 (a-b) SEM images and (c-d) TEM images of Pt/Mo₂C.

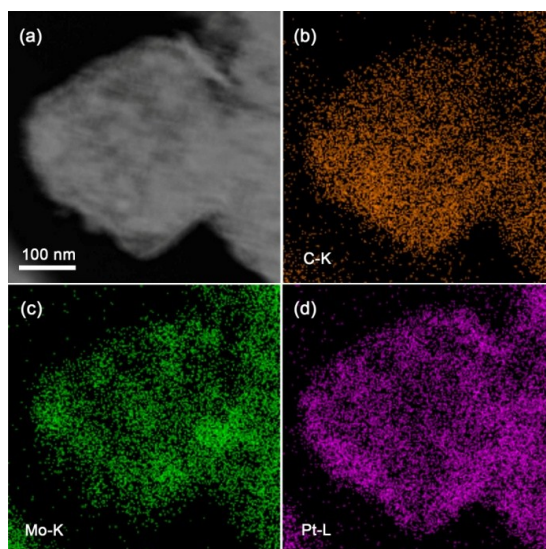


Fig. S5 HAADF-STEM elemental mapping of an individual Pt/Mo₂C nanostructure.

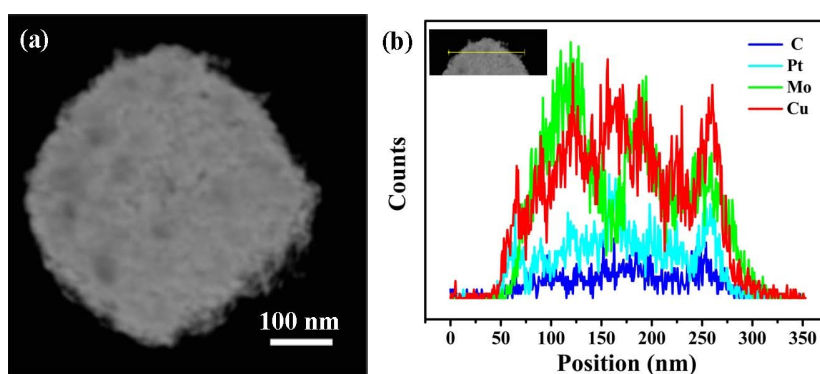
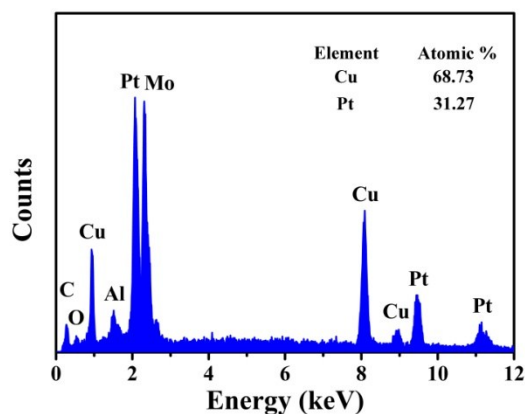
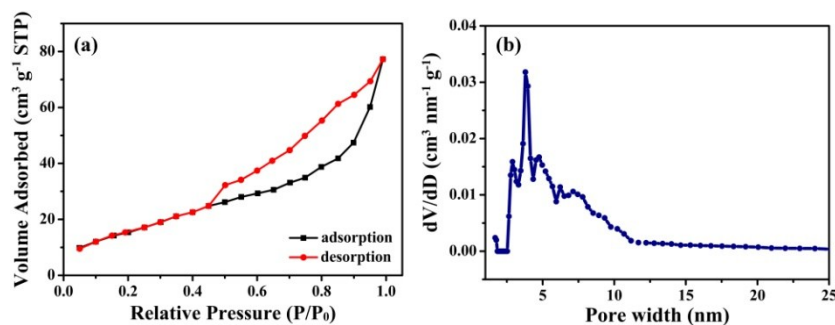
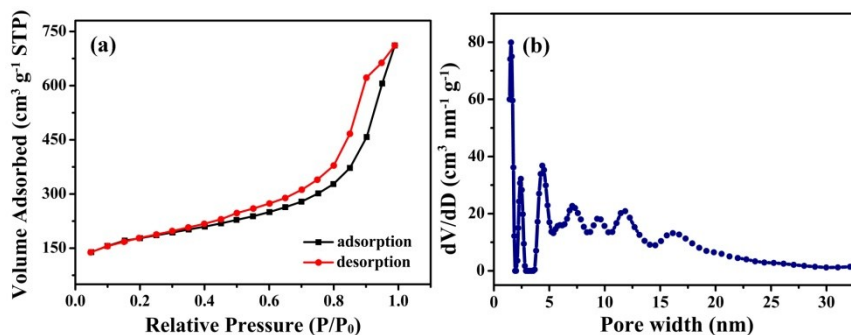


Fig. S6 (a) HAADF-STEM image and (b) line scanning profiles across a single Pt-Cu/Mo₂C nanostructure.

Table S1 Element contents (wt %) of different samples determined by ICP-OES.

Samples	Mo	Pt	Cu
Mo ₂ C	58.60	0	0.1532
Pt/ Mo ₂ C	45.38	24.42	0.1734
Pt-Cu/ Mo ₂ C	34.46	27.08	19.39

**Fig. S7** EDX spectrum of Pt-Cu/Mo₂C.**Fig. S8** (a) N₂ adsorption/desorption isotherms and (b) pore size distributions of Cu/Mo₂C.**Fig. S9** (a) N₂ adsorption/desorption isotherms and (b) pore size distributions of Mo₂C.

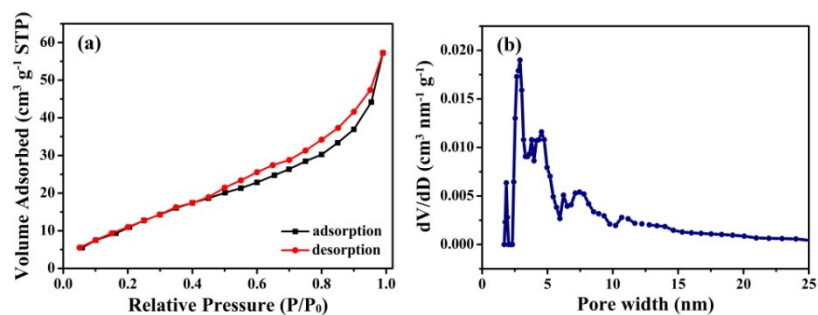


Fig. S10 (a) N₂ adsorption/desorption isotherms and (b) pore size distributions of Pt/Mo₂C.

Table S2 Comparisons of BET surface areas and average pore widths for the as-prepared catalysts.

	Mo ₂ C	Cu/Mo ₂ C	Pt/Mo ₂ C	Pt-Cu/Mo ₂ C
BET surface area (m ² g ⁻¹)	132.5	108.8	78.6	91.1
Average pore width (nm)	6.6	3.8	2.9	5.3

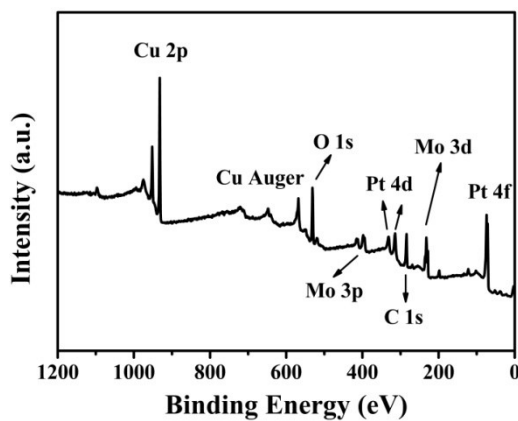


Fig. S11 XPS survey spectrum of Pt-Cu/Mo₂C.

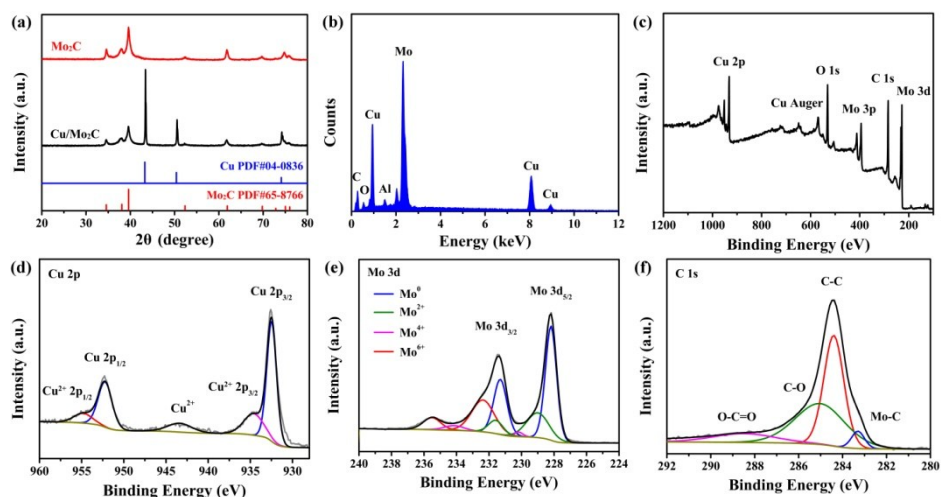


Fig. S12 (a) XRD patterns of Mo_2C and $\text{Cu}/\text{Mo}_2\text{C}$, (b) EDX spectrum, XPS spectra of (c) full survey spectrum, (d) Cu 2p, (e) Mo 3d, and (f) C 1s of $\text{Cu}/\text{Mo}_2\text{C}$.

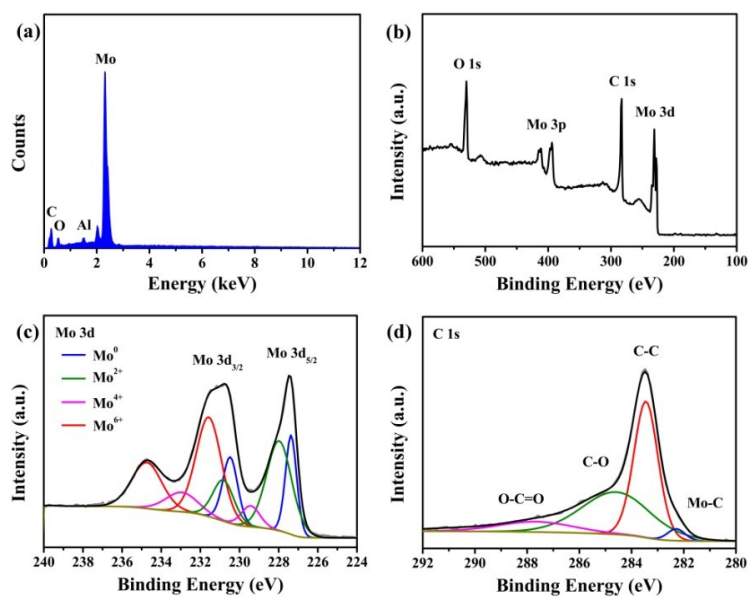


Fig. S13 (a) EDX spectrum, XPS spectra of (b) full survey spectrum, (c) Mo 3d, and (d) C 1s for Mo_2C .

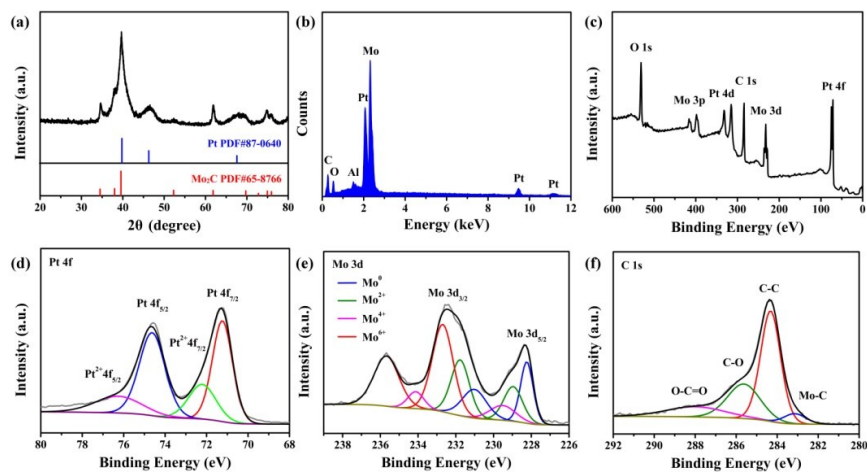


Fig. S14 (a) XRD pattern, (b) EDX spectrum, XPS spectra of (c) full survey spectrum, (d) Pt 4f, (e) Mo 3d, and (f) C 1s for Pt/Mo₂C.

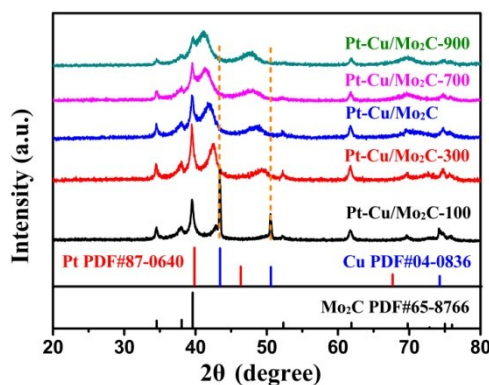


Fig. S15 XRD patterns of the samples with different Cu/Pt atomic ratios of Pt-Cu/Mo₂C.

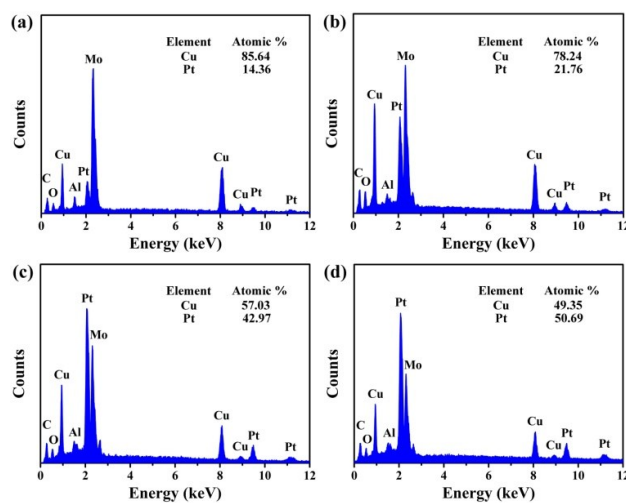


Fig. S16 EDX spectra of the samples with different Cu/Pt atomic ratios of Pt-Cu/Mo₂C.

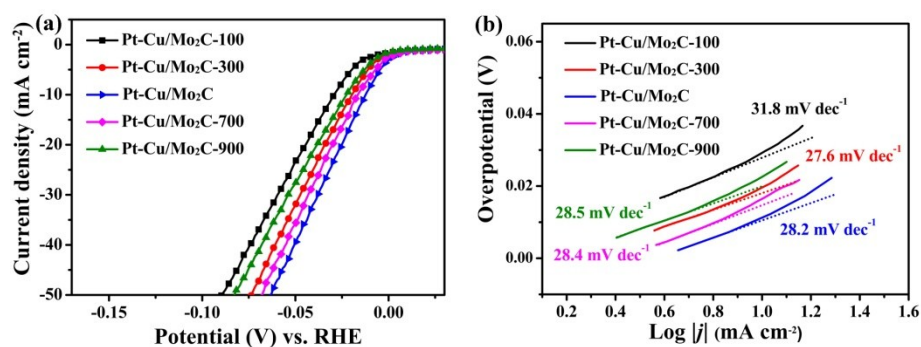


Fig. S17 (a) Polarization curves and (b) Tafel plots of the samples with different Cu/Pt atomic ratios of Pt-Cu/Mo₂C in 0.5 M H₂SO₄.

Table S3 Summary of the HER activity of the as-prepared catalysts.

Catalyst	Overpotential (mV) at 10 mA cm ⁻²	Tafel slope (mV dec ⁻¹)
Pt-Cu/Mo ₂ C-100	29.2	31.8
Pt-Cu/Mo ₂ C-300	19.6	27.6
Pt-Cu/Mo ₂ C	12.9	28.2
Pt-Cu/Mo ₂ C-700	16.3	28.4
Pt-Cu/Mo ₂ C-900	22.9	28.5

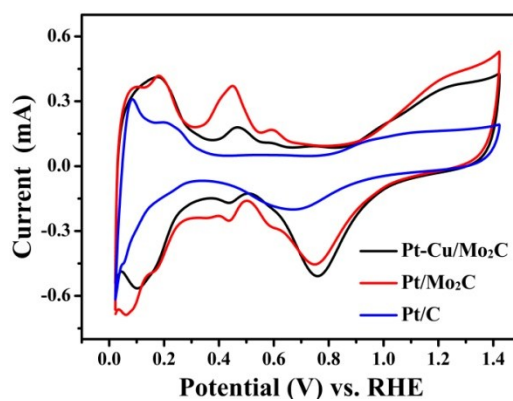


Fig. S18 CV curves of Pt-Cu/Mo₂C, Pt/Mo₂C, and Pt/C tested in N₂-saturated 0.5 M H₂SO₄ solution with a scan rate of 50 mV s⁻¹.

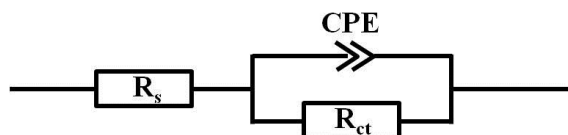


Fig. S19 Equivalent circuit used to fit the EIS data. R_s represents the overall series resistance, CPE denotes the constant phase angle element, and R_{ct} is the charge transfer resistance.

Table S4 R_{ct} values of the as-prepared samples.

Catalyst	$R_{ct} (\Omega)$
Mo_2C	1.78
$\text{PtCu}/\text{Mo}_2\text{C}$	0.58
$\text{Pt}/\text{Mo}_2\text{C}$	0.71

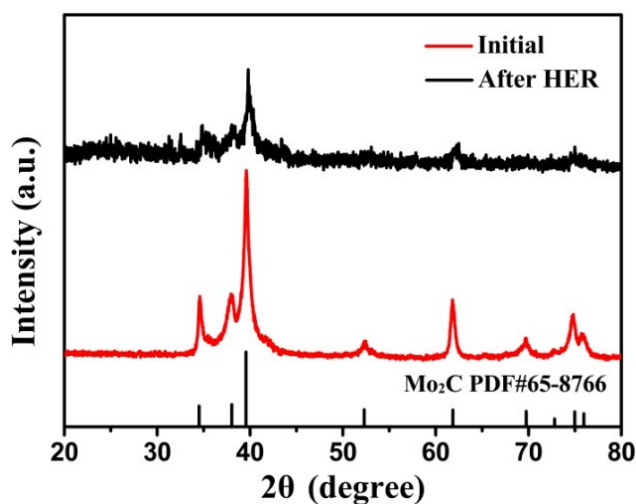


Fig. S20 XRD patterns of Mo_2C after HER test.

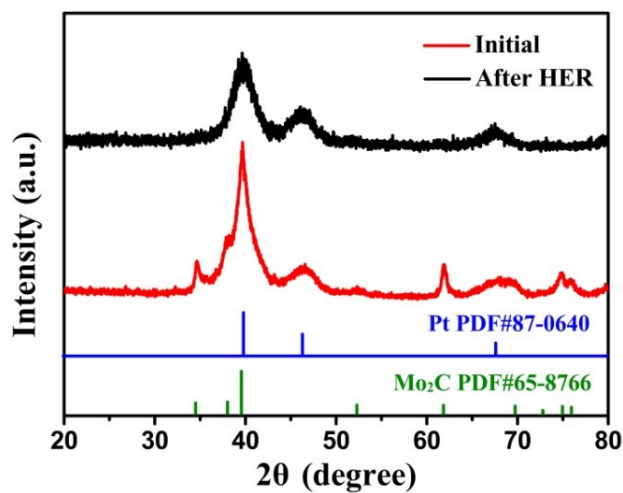


Fig. S21 XRD patterns of $\text{Pt}/\text{Mo}_2\text{C}$ after HER test.

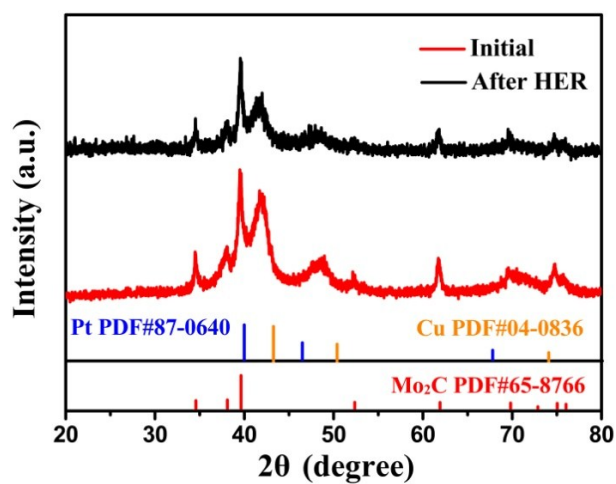


Fig. S22 XRD patterns of Pt-Cu/Mo₂C after HER test.

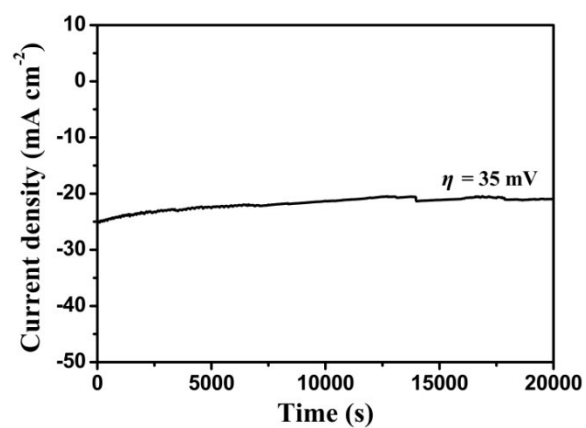


Fig. S23 I-t curves for Pt-Cu/Mo₂C at $\eta=35$ mV.

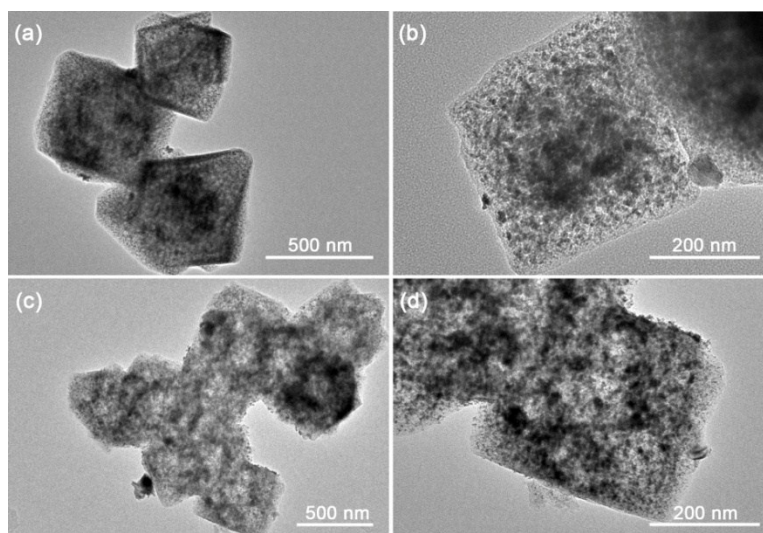


Fig. S24 TEM images of Pt-Cu/Mo₂C after i-t test. (a-b) $\eta=13$ mV; (c-d) $\eta=35$ mV.

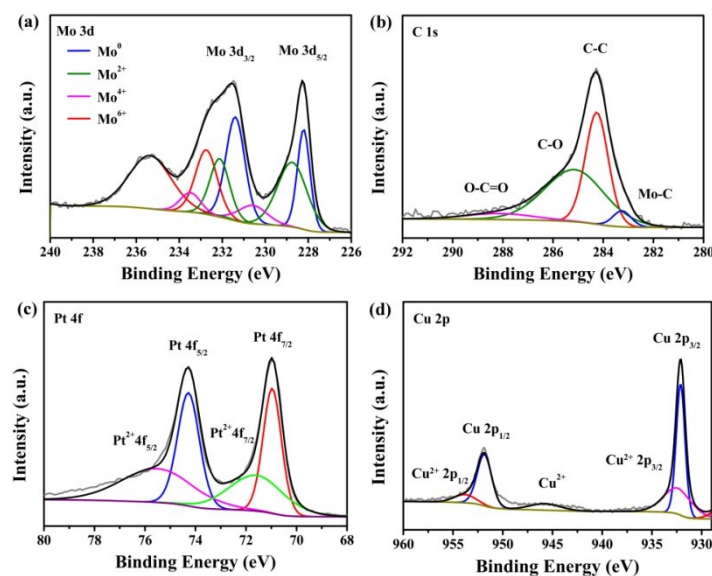


Fig. S25 XPS spectra of Pt-Cu/Mo₂C nanocomposite after HER test: (a) Mo 3d, (b) C 1s, (c) Pt 4f, and (d) Cu 2p.

Table S5 Comparison for the as-prepared catalysts and some previously reported representative HER precious metal-based electrocatalysts in 0.5 M H₂SO₄ solution.

Catalyst	Catalyst loading amount	Overpotential (mV) at 10 mA cm ⁻²	Tafel slope (mV dec ⁻¹)	Reference
Pt-Cu/Mo ₂ C	69.1 μg _{Pt} cm ⁻²	12.9	28.2	This work
Pt/Mo ₂ C	62.3 μg _{Pt} cm ⁻²	18.9	35.7	This work
Pd/Cu-Pt	41 μg cm ⁻²	22.8	25	Angew. Chem. Int. Ed., 2017, 56, 16047
PdCu@Pd NCs	140 μg cm ⁻²	68	35	ACS Appl. Mater. Interfaces, 2017, 9, 8151
NiAu/Au core/shell NPs	204 μg cm ⁻²	~36	36	J. Am. Chem. Soc., 2015, 137, 7365
Pt NCs@CIAC-121	--	48	58	J. Am. Chem. Soc., 2016, 138, 16236
RuP ₂ @NPC	230.7 μg _{Ru} cm ⁻²	38	38	Angew. Chem. Int. Ed., 2017, 56, 11559
ALD50Pt/NGNs	76.5 μg cm ⁻²	40	29	Nat. Commun., 2016, 7, 13638
Pd@PdPt	121.7 μg _{Pt} cm ⁻²	39	38	J. Mater. Chem.

400-SWNT/Pt	$\sim 190 \mu\text{g cm}^{-2}$	27	38	A, 2016, 4, 16690 ACS Catal., 2017, 7, 3121
Pt-MoS ₂	$75 \mu\text{g cm}^{-2}$	53	40	Nat. Commun., 2013, 4, 1444
PtCoFe@CN	$13.1 \mu\text{g}_{\text{Pt}} \text{cm}^{-2}$	45	32	ACS Appl. Mater. Interfaces, 2017, 9, 3596
Ru@C ₂ N	$81.8 \mu\text{g}_{\text{Ru}} \text{cm}^{-2}$	22	30	Nat. Nanotechnol., 2017, 12, 441
Pt ML/Au NF/Ni foam	--	~ 68	53	Sci. Adv., 2015, 1, e1400268
Ru-MoO ₂	$84.4 \mu\text{g}_{\text{Ru}} \text{cm}^{-2}$	55	44	J. Mater. Chem. A, 2017, 5, 5475